REGULAR ARTICLE

blood VTH
vessels, thrombosis & hemostasis

iMer, a naturally occurring MERTK splice variant, binds to GAS6 to decrease platelet activation and thrombus formation

Stephanie Springborn,[1] Samantha Judd,[1] Patricia Morateck,[1] David VanderZee,[1] Adam Kidwell,[1] Christine Brzezinski,[2] Allaura Cox,[2] Susan Sather,[2] Keith B. Neeves,[2] Deborah DeRyckere,[3] Jorge Di Paola,[4] Douglas K. Graham,[3] and Brian R. Branchford[1,2]

[1]Hematology, Thrombosis and Hemostasis Research Program, Versiti Blood Research Institute, Wauwatosa, WI; [2]Section of Hematology/Oncology/Bone Marrow Transplant, Department of Pediatrics, University of Colorado Anschutz Medical Campus, Aurora, CO; [3]Section of Hematology/Oncology/Bone Marrow Transplant, Department of Pediatrics, Emory University, Atlanta, GA; and [4]Section of Hematology/Oncology/Bone Marrow Transplant, Department of Pediatrics, Washington University St. Louis, St. Louis, MO

Key Points

- iMer, an isomer of MERTK, decreases human platelet activation and murine thrombosis but does not promote increased tail-clip bleeding.
- The activity involves direct binding of iMer to GAS6.

Unopposed platelet activation can be associated with pathologic thrombosis. An intact growth arrest–specific gene 6 (GAS6)/Mer receptor tyrosine kinase (MERTK) signaling pathway contributes importantly to potentiating platelet activation triggered by molecular agonists ex vivo and thrombus stabilization in vivo. We describe, herein, the inhibition of platelet function and stable thrombus formation conferred by iMer, a naturally occurring MERTK splice variant, that acts as a GAS6 decoy receptor and decreases phosphorylation of MERTK. Human and murine platelets incubated with this truncated protein demonstrate reduced activation in ex vivo assays including aggregometry (similar to treatment with anti-GAS6 antibody), expression of P-selectin, spreading on collagen, and accumulation on collagen at a venous shear rate. Wild-type C57BL/6 mice treated with iMer had improved survival in a collagen/epinephrine-induced pulmonary embolism model, without increase in tail bleeding time on preliminary analysis. Taken together, these findings confirm previous data suggesting the importance of GAS6-MERTK signaling in platelet activation and thrombus formation and highlighting the potential therapeutic implications of targeting this pathway as a means of treating or preventing thrombosis.

Introduction

Platelet activation is an essential component of normal hemostasis. Activated platelets release procoagulant materials from their granules and provide a phospholipid surface for thrombin burst, leading to platelet aggregation and subsequent fibrin clot formation. Unchecked platelet activation, however, can lead to pathologic thrombosis. Thromboembolic conditions, comprising arterial (ischemic heart disease and stroke) and venous (deep vein thrombosis and pulmonary embolism) events accounted for ~1 in 4 deaths worldwide, according to data from the Global Burden of Diseases, Injuries, and Risk Factors Study 2010.[1]

Platelet activation responses include a signal transduction pathway involving the platelet-surface protein tyrosine kinase (TYRO3)/receptor tyrosine kinase (AXL)/Mer receptor tyrosine kinase (MERTK; TAM) family of receptors and their primary vitamin K–dependent ligands growth arrest–specific gene 6 (GAS6) and protein S (PROS1).[2,3]

Submitted 21 June 2024; accepted 1 April 2025; prepublished online 26 May 2025; final version published online 19 August 2025. https://doi.org/10.1016/j.bvth.2025.100078.

Original data are available on request from the corresponding author, Brian R. Branchford (bbranchford@versiti.org).

The full-text version of this article contains a data supplement.

The TAM receptors comprise 2 immunoglobulin-like and 2 fibronectin type III repeats in their extracellular domains in tandem. This is connected to a single-pass transmembrane domain and a cytoplasmic protein tyrosine kinase. Upon ligand binding, the receptor dimerizes and the tyrosine kinase becomes activated.[4] Activated TAM receptors stimulate hemostasis by facilitating platelet stabilization via activation of the αIIb/β3 integrin.[5,6]

The primary phosphorylation site on MERTK is tyrosine 867, which is considered the autophosphorylation docking site responsible for activating downstream signaling pathways upon MERTK activation by ligand binding.[7] MERTK is predominantly expressed in the ovaries, testes, prostate, lungs, and kidneys, and to a lesser extent in the thymus, spleen, liver, small intestine, colon, and placenta.[8] MERTK is located on the surface of platelets and mediates thrombogenesis and platelet stabilization after integrin activation, granule secretion, and platelet aggregation through platelet-to-platelet contact.[8] Without this mechanism, platelet plugs disaggregate prematurely.[9] Important downstream mechanisms in platelets include increased granule secretion, activation of phosphoinositide 3-kinase, and phosphorylation of β_3 integrin, leading to an increase in outside-in signaling via the αIIbβ3 integrin.[8] GAS6 is a 75-kDa vitamin K–dependent protein with similar modular composition to, and high structural homology (~42%) with, protein S. Its thrombin-sensitive region (a disulfide-bridged thumb loop) is not susceptible to cleavage by the action of serine proteases, so there is likely no interaction with protein C for direct anticoagulant effect. GAS6 is produced primarily in the heart, kidneys, and lungs, and to a mild degree in the liver, and circulates in the plasma with a concentration of ~20 to 50 ng/mL (0.25 nmol/L). Tissues in which Gas6 is expressed include endothelial cells, bone marrow, and platelets. Although Gas6 binds the TAM receptors with different affinities, with AXL similar to or slightly higher than TYRO3, both of which are much higher than for MERTK,[10] MERTK is the most abundant of the TAM receptors on human and mouse platelets.[11]

GAS6-MERTK signaling enhances the platelet activation necessary for primary hemostasis.[8] Upon vessel injury, vascular GAS6 also upregulates endothelial cell tissue factor expression, enhancing activation of the extrinsic pathway of fibrin clot formation (secondary hemostasis). In previous studies, deficiencies of either GAS6 or ≥1 of the TAM receptors inhibited platelet activation signaling and thrombus formation in mice.[5] Similarly, the small-molecule MERTK inhibitor, UNC2025, decreased platelet activation in vitro, and thrombus formation in vivo.[12] Plasma-soluble TAM receptor extracellular domains, such as sMer and sAxl, created via cleavage of cell-surface receptors by specific metalloproteinases, also decrease platelet activation and thrombosis, likely by acting as decoy receptors to bind available GAS6 in the circulation.[13]

Although GAS6 levels are known to increase in adult humans as acute phase reactants during times of physiologic stress,[14-16] the mechanisms underlying subsequent regulation of this signaling pathway are not well understood. The initial analysis of MERTK in hematopoietic cells and cell lines indicated the presence of 2 different polymerase chain reaction (PCR) products, 1 of which was MERTK at 526 base pairs (bp) and another 1 at 578 bp, suggesting an alternative splice product with a 52-bp insertion.[17] Here, we describe, to our knowledge for the first time, an alternatively spliced isomer (iMer) of the MERTK receptor that binds to GAS6, decreasing platelet activation in vitro and thrombus formation in vivo. The function of iMer as a decoy receptor was predicated upon the similar previously reported activity of sMer and sAxl.

Materials and methods

Ethical approvals

Blood collection. Human whole blood (WB) was collected by venipuncture with informed consent from healthy volunteers under institutional review board-approved protocols Colorado Multiple Institutional Review Board number 09-0816 and Versiti institutional review board number PRO00048877.

Animal thrombosis models. All experiments were approved by pertinent institutional animal care and use committees: University of Colorado institutional animal care and use committee number 05001 and Medical College of Wisconsin animal use agreement number 00007467.

Agonists and inhibitors

iMer. Primers were used to amplify transcripts for full-length MERTK and the iMer isoform. Expression and purification of iMer was provided by the commercial biology contract organization GenScript (Piscataway, NJ). First-strand complementary DNA (cDNA) was prepared using Moloney murine leukemia virus reverse transcriptase in room temperature (RT) buffer (50 mM Tris-HCl [pH 8.3], 75 mM KCl, 10 mM dithiothreitol, and 3 mM $MgCl_2$), 15 units of RNA guard (Pharmacia), 10 pmol of random hexamers, and 1.25 mM of each 2′-deoxynucleoside 5′-triphosphate in a 20-μL reaction mixture. The volume of the cDNA was adjusted to 25 to 60 μL with Tris EDTA after first-strand synthesis. First-strand cDNA (5 μL) was amplified in a 50-μL volume of PCR buffer (10 mM Tris-HCl [pH 9.0], 50 mM KCl, 1.5 mM $MgCl_2$, 0.01% gelatin, and 0.1% Triton X-100), 0.2 mM of each 2′-deoxynucleoside 5'-triphosphate, 50 pmol of each primer, and 2.5 units of Taq DNA polymerase (Gibco Bethesda Research Laboratories). To test for the integrity of the RNA samples and for template standardization, amplification by PCR using actin primers (HACA-1F and HACA-1R) was performed under the following conditions: 5 minutes at 94°C, 1 minute at 55°C, and 2 minutes at 72°C (1 cycle); 1 minute at 94°C, 1 minute at 55°C, and 2 minutes at 72°C (22 cycles); and 1 minute at 94°C, 1 minute at 55°C, and 10 minutes at 72°C (1 cycle). Transcription of iMer in samples was demonstrated using primers 3F, 51F, RINS, and 2R. The sequences of these primers are as follows: 51F 5′-GATGATGAAGTTACAGCAAT-3′, 3F 5′-CACCTCTGCCTTACCACATCT-3′, RINS 5′-GGAGTCAACAGTAGAAGAGAG-3′, 2R 5′-ATCCACAAAAGCAGCCAAAGA-3′. Each PCR contained a reverse transcriptase negative control, a no-template control, and a positive control. The PCR products were analyzed by electrophoresis of 10 μL of each reaction mixture on a 1.0% agarose gel containing ethidium bromide. Expression of the iMer protein was performed in a HEK293 cell system with purity reported as 85% to 90% in the lots used for this work and resuspended in phosphate-buffered saline (PBS). iMer (calculated molecular weight of ~40 kDa) was detected with estimated molecular weight of 65 to 94 kDa (differentially glycosylated forms) based on sodium dodecyl sulfate–polyacrylamide gel electrophoresis (SDS-PAGE) and western blot analysis under reducing conditions, as seen in supplemental Figure 1C.

PRP and washed platelet (WP) preparation. WB was drawn from healthy volunteers into 3.8% sodium citrate, as previously described,[18,19] with addition of acid-citrate-dextrose. Platelet-rich plasma (PRP) was prepared by centrifugation at 150*g* for 7 minutes at RT. Platelets were pelleted by centrifuging PRP at 1100*g* for 18 minutes in the presence of prostacyclin (0.1 mg/mL; Sigma-Aldrich, St. Louis, MO), and resuspended in modified Tyrode buffer (129 mM NaCl, 0.34 mM Na_2HPO_4, 2.9 mM KCl, 12 mM $NaHCO_3$, 20 mM HEPES [*N*-2-hydroxyethylpiperazine-*N*′-2-ethanesulfonic acid], 5 mM glucose, and 1 mM $MgCl_2$; pH 7.3) with acid-citrate-dextrose, after supernatant was discarded. The solution was spun again at 1100*g* for 10 minutes with 0.1 mg/mL prostacyclin and resuspended in buffer to desired concentration after discarding the supernatant.

PRP and platelet lysate preparation. WB was drawn from healthy volunteers into 3.8% sodium citrate as previously described.[15,16] PRP was obtained via centrifugation at 150*g* for 10 minutes at RT. Remaining plasma and cells were centrifuged at 1100*g* for 18 minutes at RT to obtain platelet-poor plasma (PPP). PRP platelet concentration was determined on a Heska Element HT5 and then diluted to 250 × 10^3/μL via addition of PPP. Platelets were then pelleted via centrifugation at 1100*g* for 10 minutes at RT. Supernatant was removed, and platelets were resuspended in lysis buffer (HEPES 50 mM, NaCl 150 mM, EDTA 10 mM, glycerol 10% by volume, Triton X-100 1% by volume, and protease inhibitory cocktail [10 μL/mL of buffer; catalog no. 539131; Calbiochem]), pelleted via centrifugation, and resulting supernatant was aliquoted then stored at −80°C. Remaining PPP was stored at −80°C.

MERTK phosphorylation assay. A total of 697 human leukemia cells were cultured in RPMI 1640 without serum and incubated with 1 μM iMer or PBS for 10 minutes, then stimulated with 200 nM recombinant human (rh) Gas6 (catalog no. NP_000811; R&D Systems, Minneapolis, MN) for 10 minutes. Pervanadate solution was prepared fresh and cultures were treated with 120 mM pervanadate to stabilize phosphorylated MERTK before preparation of whole-cell lysates, as previously described.[13] Lysates were incubated with anti-MERTK antibody (catalog no. MAB8912; R&D Systems) and protein G Sepharose beads (Invitrogen), and recovered proteins were resolved by SDS-PAGE. Phosphorylated and total MERTK were detected by immunoblot, as previously described.[13]

iMer/GAS6 binding assays. A mixture of 200 nM iMer (GenScript) and 1 mg biotinylated anti-human MERKTK immunoglobulin G (catalog no. BAF891; R&D Systems), both diluted in PBS-Tween (PBST) buffer containing 2% bovine serum albumin (BSA), were incubated with shaking for 30 minutes. Washed Dynabeads MyOne Streptavidin T1 beads (catalog no. 65601; Thermo Fisher Scientific) were added, and complexes were incubated with shaking for an additional hour. Varying doses of GAS6 (catalog no. H00002621-P01; Abnova) and $CaCl_2$ (5 mM final concentration in 2% BSA in PBST), were then added followed by an additional incubation with shaking for 1 hour. Beads were magnetically immobilized and washed 3 times with 1 mL PBST containing 2% BSA. Bound proteins were subjected to SDS-PAGE and immunoblotted with anti-human GAS6 antibody (catalog no. sc376087; Santa Cruz Biotechnology, Dallas, TX).

Respectively, 200 nM GAS6 (catalog no. H00002621-P01; Abnova) and 1 mg biotinylated anti-human GAS6 immunoglobulin G (catalog no. BAF885; R&D Systems), both diluted in PBST buffer containing 2% BSA were incubated with shaking for 30 minutes. Washed Dynabeads MyOne Streptavidin T1 beads (catalog no. 65601; Thermo Fisher Scientific) were added, and complexes were incubated with shaking for an additional hour. Varying doses of iMer (GenScript)) and $CaCl_2$ (5 mM final concentration in 2% BSA in PBST), were then added followed by an additional incubation with shaking for 1 hour. Beads were magnetically immobilized and washed 3 times with 1 mL PBST containing 2% BSA. Bound proteins were subjected to SDS-PAGE and immunoblotted with anti-human MERTK antibody (catalog no. ab52968; Abcam).

Immunoprecipitation and western blot of endogenous iMer. Platelet lysate and PPP were incubated at RT with 1 μg of anti-mer (catalog no. BAF 891; R&D Systems) for 2 hours with agitation on a Labquake shaker (model C400110). Dynabeads MyOne Streptavidin T1 (10 μL; catalog no. 65601; Thermo Fisher Scientific) were magnetically immobilized and washed 3 times with PBS and added to the sample-antibody mixture and incubated at RT for 1 hour with agitation on a Labquake shaker. Bead-antibody-protein complexes were then magnetically immobilized, washed, and resuspended 3 times with PBS with 0.05% Tween. Bound proteins were eluted and subjected to SDS-PAGE and subsequent immunoblotting with anti-MER antibody (catalog no. ab52968; Abcam).

Platelet aggregation. PRP and/or WPs were prepared as described earlier and incubated for 8 minutes with vehicle control (1× PBS) or 5 μM iMer in 1× PBS. Samples were analyzed by a light transmission aggregometer after stimulation by 0.25 to 0.5 μg/mL collagen or 1 to 2 mM adenosine 5′-diphosphate (ADP). Maximal aggregation (percent) was recorded. GAS6 (0.28-2 nM; catalog no. 885-GSB; R&D Systems) was used to reverse the iMer-induced inhibition. Anti-GAS6 antibody (1:1000; catalog no. sc-376087; Santa Cruz Biotechnology) was used to directly block GAS6 activity. Variable aggregation response in the presence of rhGAS6 was expected because native GAS6 is an acute phase reactant and likely exists at a range of levels in our cohort of blood donors based upon their inflammatory state at the time of the donation. Elevated circulating GAS6 levels would likely augment platelet activation at lower ADP concentrations rather than lower circulating GAS6 levels. We, therefore, elected to perform these experiments with a dose of ADP necessary to achieve ~80% platelet activation with agonist alone, although this dose of ADP varied among individuals and even within the same individual on different days.

Microfluidic flow assay. Equine tendon fibrillar type 1 collagen was purchased from Chrono-log Corp (Havertown, PA). The collagen was diluted to 500 μg/mL in a 5% glucose solution and patterned in a 100 × 50 μm strip in a polydimethylsiloxane microfluidic channel onto a glass slide for 1 hour. After collagen patterning, the slide was blocked with 1 mg/mL BSA for 1 hour at RT. A second polydimethylsiloxane microfluidic flow device was mounted perpendicularly to the collagen strip.[20,21] WB from healthy human volunteers was drawn with a 27-gauge needle into citrate and corn trypsin inhibitor, incubated for 15 minutes with either NaCl, 1 μM iMer in NaCl, or 2 μM abciximab in NaCl, and then treated with fluorescein isothiocyanate–conjugated mouse

antihuman CD41a (HIP8 monoclonal antibody; BD Biosciences, Franklin Lakes, NJ) at a ratio of 1:1000. The flow device and slide were placed on an inverted microscope (40×; IX81; Olympus, Waltham, MA). WB (100 μL) was recalcified and pulled through the channels at a wall shear rate of 650 s^{-1} by syringe pump (Harvard Apparatus, Holliston, MA) for 3 minutes, and platelet aggregation was captured in real time[20,22] using an Orca Flash4 CMOS camera (Orca-ER; Hamamatsu) and cellSens imaging software (Olympus Life Science). An image was captured every 1 second over the duration of the experiment. After 3 minutes, the channel was washed through with Tyrode's buffer while continuously capturing images in real time. Surface area coverage and aggregate size for each series was determined using the National Institutes of Health ImageJ plugin.

Flow cytometric analysis. Human WPs (200 × 10^3/μL) were prepared as described earlier and incubated with vehicle control (NaCl) or 1 μM iMer in NaCl (data not shown) for 10 minutes at 37°C, after which time platelets were stimulated with thrombin (0.5 U/mL) for 10 minutes at 37°C. Anti-CD41 (BD Biosciences) and anti–P-selectin (BD Biosciences) antibodies were added, and the solution was incubated, fixed with paraformaldehyde, and analyzed by FC-500 flow cytometer (Beckman Coulter) and FlowJo software (version 10).

Platelet spreading. Human WPs were prepared as described earlier and incubated with PBS (negative control), 1 μM iMer, or 2 μM abciximab (positive control) for 10 minutes, seeded on 100 μg/mL collagen-coated glass coverslips at 2 × 10^4/μL, incubated for 15 minutes, fixed, and dried. Coverslips were then mounted and imaged with a field emission scanning electron microscope at 1000× to 5000× magnification after gold sputtering. Ten fields per sample were viewed, and representative images were chosen. A Japan Electron Optics Laboratory field emission scanning electron microscope (Peabody, MA) was used for imaging at 1000× and 5000× magnification.

Murine pulmonary embolism model. Six- to 12-week-old C57BL/6J mice were anesthetized.[13,23] Collagen (0.28 mg/kg) and epinephrine (0.029 mg/kg) were injected IV 15 minutes after injection of either 60 mg/kg iMer[24] or equivalent volume of PBS vehicle, and time to breathing cessation was noted. Mice still alive 15 minutes after collagen/epinephrine injection were euthanized.

Tail-clip bleeding assay. Saline vehicle or 60 mg/kg iMer was injected into the retro-orbital sinus of anesthetized wild-type mice and allowed to circulate for 15 minutes while the animal was placed in prone position on a heat block set to 37°C. Tails were snipped at a consistent diameter of 1.59 mm, using a Staedtler circle template and the proximal ends were placed in a conical tube containing 37°C normal saline for 15 minutes. Total bleeding time (including rebleeds) was recorded and compared to that of GAS6 knockout mice.

Statistical analysis

Statistical analyses were conducted using GraphPad Prism (version 10; GraphPad Software Inc, La Jolla, CA). Not all data could be confirmed as normally distributed by D'Agostino-Pearson or Shapiro-Wilk tests, even after removal of statistical outliers as identified by robust regression and outlier removal analysis (Q = 5%), so were expressed as median values with interquartile range (IQR) and were evaluated using an unpaired Mann-Whitney *U* rank-sum test for continuous variables whose distribution may be artificially affected by set experimental cutoff end point times. Other values were compared using Wilcoxon signed pairs rank test.

Results

iMer is expressed in gastrointestinal, genitourinary, endocrine, and lymphatic tissues and inhibits phosphorylation of MERTK by GAS6

Sequencing of the alternative splice product demonstrated insertion of an additional exon, 7A, between exons 7 and 8. Exon 7A contains an in-frame stop codon, leading to production of a truncated MERTK protein with 2 immunoglobulin domains and 1 FNIII domain (supplemental Figure 1). Gene expression analysis demonstrated both iMer and full-length MERTK transcripts in various body tissues (Figure 1A). We hypothesized that, like sMer, iMer would act as a GAS6 decoy receptor. Indeed, MERTK was phosphorylated (ie, activated) in 697 human acute leukemia cells in the presence of GAS6 (Figure 1B). In contrast, incubation with iMer reduced phosphorylation of MERTK in response to GAS6. We demonstrated all 3 known MERTK isoforms, full-length cMer receptor, soluble MERTK extracellular domain sMer, and the present compound iMer, in platelets as demonstrated in Figure 1C.

iMer binds GAS6 in a dose-dependent fashion

Figure 2, representative of 3 independent assays, demonstrates that iMer and GAS6 bind directly in coimmunoprecipitation and the relationship is concentration dependent. glutathione S-transferase–tagged GAS6/iMer complexes were detected by immunoprecipitating with anti-human MERTK antibody and immunoblotting with an anti-human GAS6 antibody. GAS6/iMer complexes were also detected when immunoprecipitated with anti-human GAS6 antibody and immunoblotting with anti-human MERTK antibody. His-tagged GAS6 (200 nM) or 200 nM each GAS6 and iMer were immunoprecipitated with anti-human GAS6 antibody. iMer coimmunoprecipitates with the GAS6 and is detected with anti-human MERTK antibody. iMer (200 nM) or 200 nM each iMer and GAS6 were immunoprecipitated with anti-human MERTK antibody. GAS6 coimmunoprecipitates with the iMer and is detected with anti-human GAS6 antibody.

iMer inhibits platelet aggregation induced by low-dose ADP in human PRP

GAS6 does not activate platelets alone (data not shown) but rather serves to augment the signaling of other platelet agonists.[5,25] This effect is most visible when using weaker agonists such as low-dose ADP. Aggregation tracings demonstrated decreased aggregation over time for platelets in human PRP treated with 5 mM iMer compared with vehicle control after activation with 1 to 2 mM ADP (Figure 3A), with a significant reduction in median final aggregation from 90% (IQR, 86%-95%; n = 4) for platelets incubated with vehicle control to 33% (IQR, 29%-40%; $P < .05$) after treatment with iMer (Figure 3B). Addition of rhGAS6 was sufficient for partial recovery of platelet aggregation in PRP pretreated with iMer before addition of ADP (Figure 3C). Median final aggregation was significantly decreased from 87% (IQR, 85%-90%) for platelets incubated with

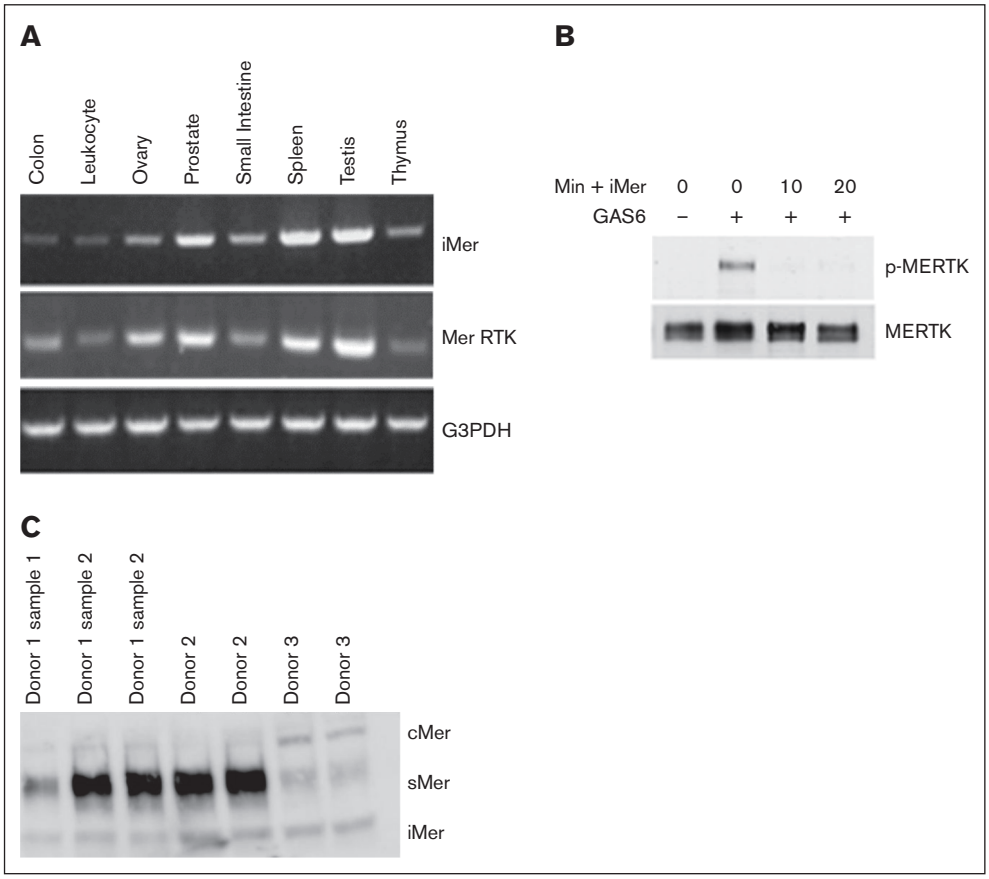

Figure 1. iMer is expressed in gastrointestinal, genitourinary, endocrine, and lymphatic tissues, and inhibits phosphorylation of MERTK induced by GAS6. (A) iMer and full-length MERTK transcripts were detected by reverse transcription PCR, with G3PDH as loading control, from C57BL/6 wild-type mouse tissue. (B) A total of 697 cells treated with vehicle control or with iMer for 10 or 20 minutes as indicated were cultured with or without 200 nM GAS6 to activate MERTK receptor. MERTK was then immunoprecipitated. Phosphorylated (denoted by p-MERTK) and total MERTK proteins were detected by immunoblot. Images shown are representative of 2 independent experiments. (C) Mer isoform prevalence in platelets varies among individuals. Immunoblot of platelet lysates collected from 3 donors, 1 of whom had multiple samples collected across different days. The blots demonstrate full-length MERTK (cMer), soluble MERTK extracellular domain (sMer), and iMer. G3PDH, glyceraldehyde-3-phosphate dehydrogenase.

vehicle control to 29% (IQR, 29%-32.5%; $P < .05$) after treatment with iMer alone and was restored to 56% (IQR, 47%-71%) when excess rhGAS6 was added (Figure 3D). Similar results were obtained when GAS6 antibody was used to titrate GAS6. Aggregation tracings showed decreased aggregation over time after activation with ADP in PRP for platelets treated with GAS6 antibody compared with vehicle control, with partial rescue of aggregation in response to addition of excess GAS6 (Figure 3E). Median final aggregation was 88% (IQR, 46.25%-99%) for platelets incubated with vehicle control compared with 7% (IQR, 5%-18%) for platelets incubated with GAS6 antibody and 20.5% (IQR, 8.25%-82.25%) after incubation with GAS6 antibody and excess GAS6 (Figure 3F). Exogenous rhGAS6 appears to enhance ADP-induced human platelet aggregation. Human PRP samples were incubated at 37°C for 10 minutes with either rhGAS6 or saline control and aggregation was induced by 2 mM ADP (n = 3; P = not significant [ns]) as seen in supplemental Figure 4.

iMer does not inhibit platelet aggregation in human PRP in the absence of GAS6

GAS6 was depleted from human PRP by immunoprecipitation before analysis of platelet aggregation and no significant difference in maximum aggregation in samples treated with iMer (median, 74% [IQR, 62%-84.5%]) compared with vehicle control (median, 86% [IQR, 70%-86.5%]; P = ns) was observed (Figure 4). From these results, we concluded that iMer's effect on inhibiting platelet aggregation after ADP stimulation is dependent upon the presence of GAS6.

iMer inhibits platelet granule release stimulated by thrombin

Human WPs were exposed to 0.5 U/mL thrombin after incubation with iMer or vehicle control. Treatment with iMer significantly decreased P-selectin on platelets after activation with thrombin compared with platelets treated with vehicle control (Figure 5).

iMer inhibits stable aggregate formation under physiologic shear conditions

In microfluidic experiments in which human WB was infused at venous shear rate (750 s^{-1}) across a fibrillar collagen strip, vehicle-treated samples exhibited significantly higher surface area coverage (median, 9.5% [IQR, 6%-11.55%]) than samples pretreated with iMer (median, 0.9% [IQR, 0.45%-3.5%]; n = 7; $P < .01$; Figure 6A). Human

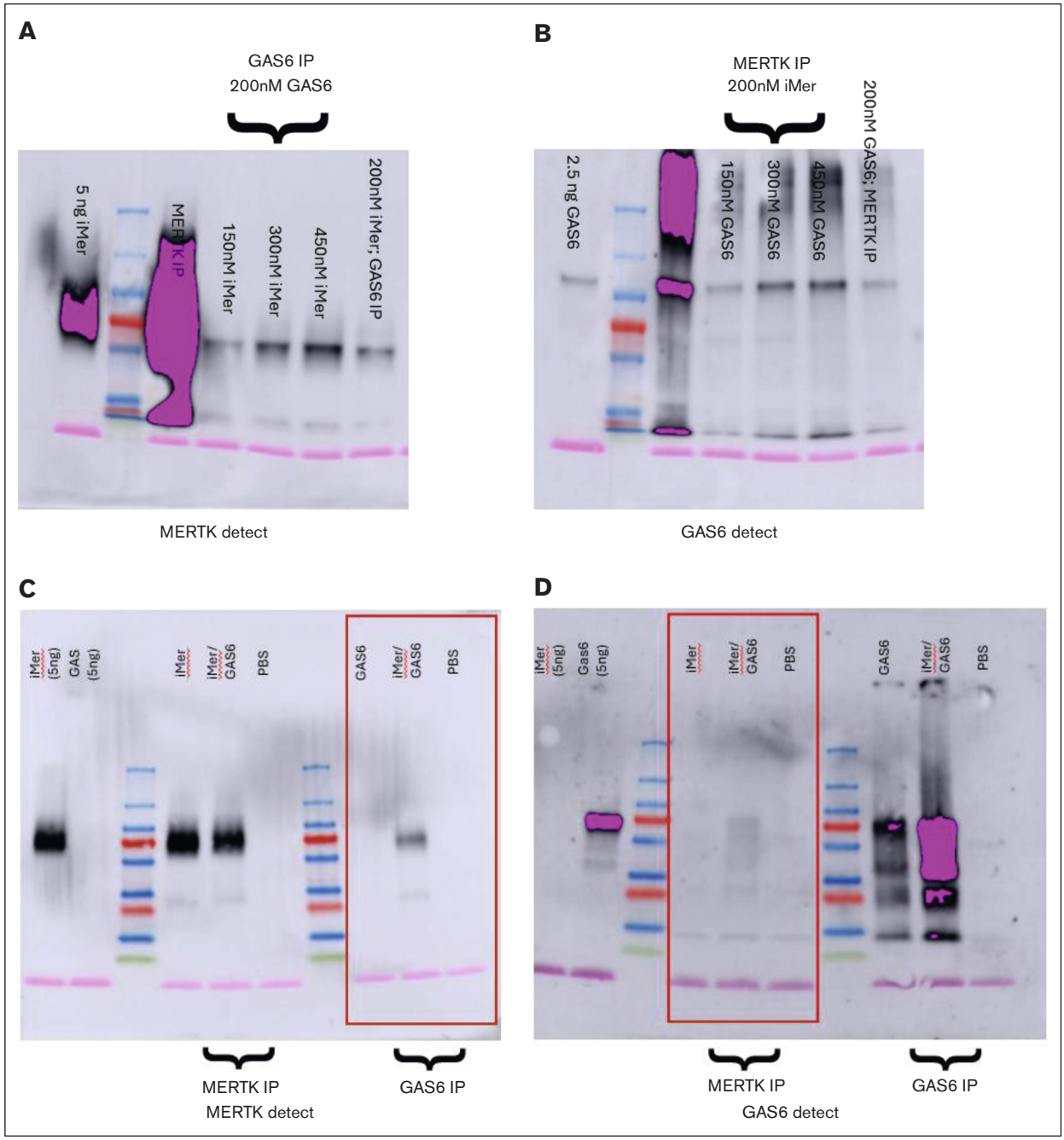

Figure 2. iMer and GAS6 bind directly in coimmunoprecipitation. Brackets depict protein added and blots are labeled by detection antibody as anti-MERTK (MERTK detect) or anti-GAS6 (GAS6 detect) as indicated. (A) Glutathione S-transferase–tagged GAS6/iMer complexes were detected by immunoprecipitating with anti-human MERTK antibody and immunoblotting with an anti-human GAS6 antibody. (B) Respectively, GAS6/iMer complexes were also detected when immunoprecipitated with anti-human GAS6 antibody and immunoblotting with anti-human MERTK antibody. Also shown are the input protein and same protein immunoprecipitation/immunoblot controls. (C) His-tagged GAS6 (200 nM) or 200 nM each GAS6 and iMer were immunoprecipitated with anti-human GAS6 antibody. iMer coimmunoprecipitates with the GAS6 and is detected with anti-human MERTK antibody. Also shown are control immunoprecipitations with anti-human MERTK and input iMer. (D) Respectively, 200 nM iMer or 200 nM each iMer and GAS6 were immunoprecipitated with anti-human MERTK antibody. GAS6 coimmunoprecipitates with the iMer and is detected with anti-human GAS6 antibody. Also shown are the control immunoprecipitations with anti-human GAS6 and input GAS6. Images are representative of 3 independent assays. IP, immunoprecipitation.

WPs, compared on brightfield image taken at the end of each microfluidic run, contained a higher proportion of small aggregates (1-2 and 3-10 platelets per aggregate) after pretreatment with iMer (median, 54% [IQR, 48%-68%] and 36% [IQR, 26.5%-36.5%], respectively; n = 7) than those pretreated with vehicle control (median, 43% [IQR, 34.5%-45.0%] and 31% [IQR, 23.5%-39%],

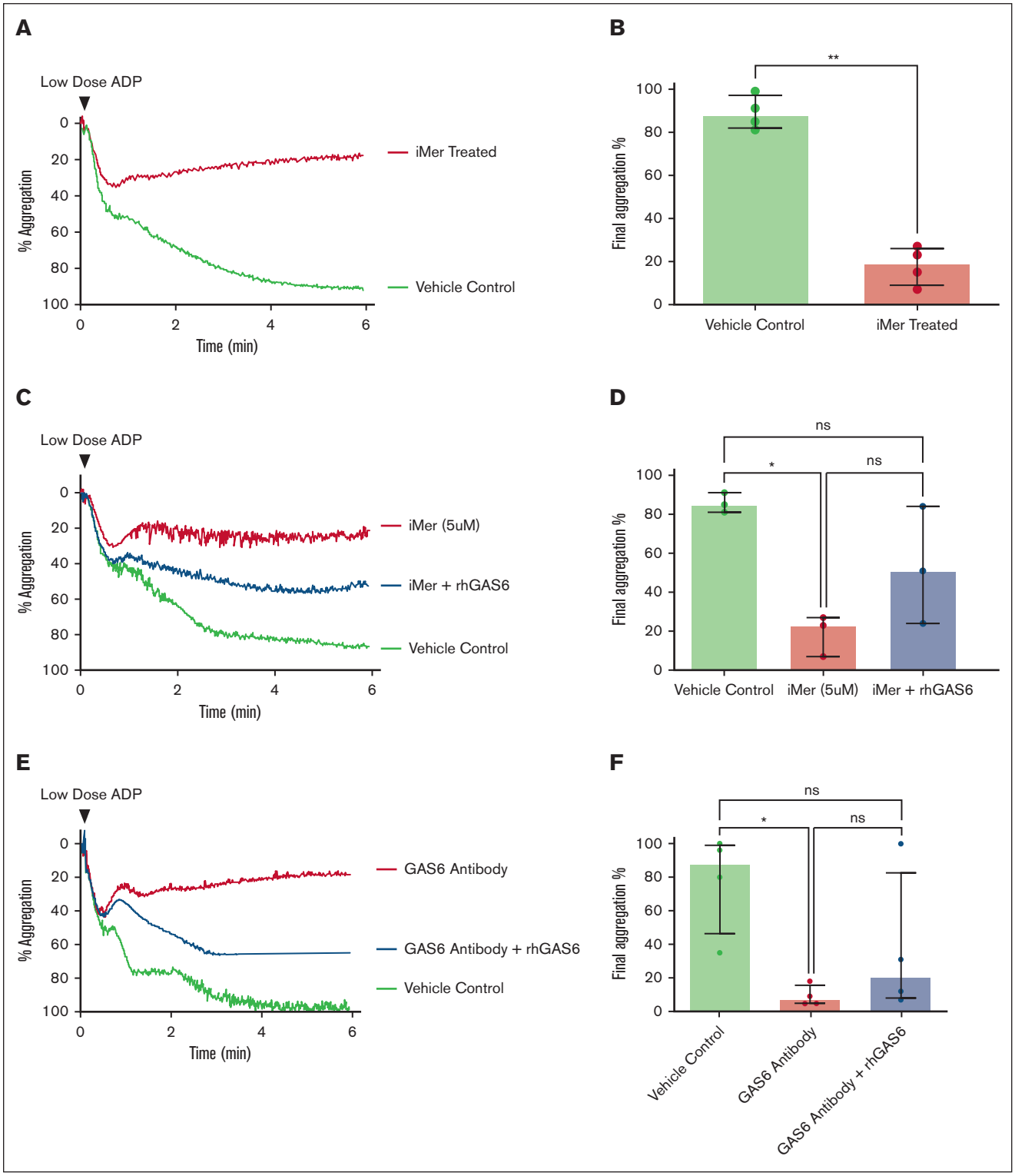

Figure 3. Removal of circulating GAS6 by addition of either iMer or anti-GAS6 antibody dampens ADP-induced platelet aggregation. (A) Representative light transmission aggregometry tracings showing inhibition of 1 to 2 mM ADP-induced platelet aggregation in human PRP in the presence of 5 μM iMer (red) or vehicle control (green). Tracings are representative of 2 to 4 independent experiments. (B) Quantitation of 4 independent experiments, median value and interquartile range are shown; $^{**}P < .01$, Wilcoxon signed pairs rank test. (C) Representative tracings showing ADP-induced platelet aggregation in the presence of 5 μM iMer (red), vehicle control (green), or 5 μM iMer plus rhGAS6 (blue). Addition of excess GAS6 can partially overcome iMer-mediated inhibition. (D) Summary of 3 experiments; $^{*}P < 05$ for control vs iMer-treated; nsfor other comparisons. (E) Representative tracings of ADP-induced platelet aggregation in the presence of GAS6 antibody (red), vehicle control (green), and GAS6 antibody plus rhGAS6 (blue). (F) Summary of 4 separate experiments, $P < .05$ for control vs anti-GAS6 antibody treatment; $P =$ ns for other comparisons, Friedman test.

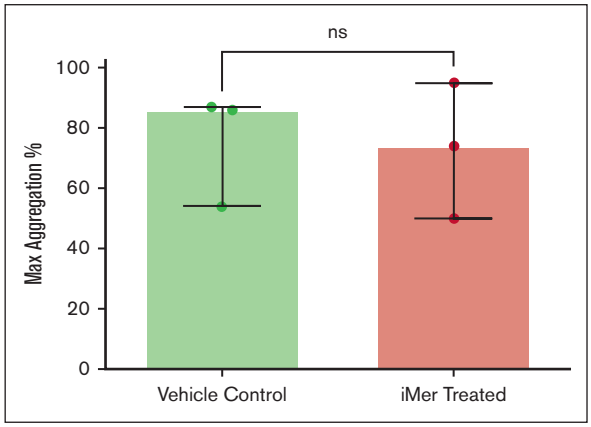

Figure 4. Platelet aggregation is not affected by treatment with iMer in the absence of GAS6. Human PRP was treated with antibody to deplete GAS6 and then incubated with 5 μM iMer (red) or vehicle control (green) before platelet activation was stimulated with 1 to 2 mM ADP. Median values and error bars denoting IQR from 3 experiments are shown (P = ns, Wilcoxon signed pairs rank test).

respectively; n = 7; P = ns). In contrast, higher proportions of large aggregates (11-50 and 50-100 platelets per aggregate) were seen in the vehicle control–treated samples (median, 17% [IQR, 14%-23.5%] and 6% [IQR, 3%-10%], respectively; n = 7; P = ns) than those pretreated with iMer (media, 14% [IQR, 0%-15%] and 0% [IQR, 0%-0%]; n = 7; P = ns). Aggregates with >100 platelets were only observed in vehicle-treated samples, consistent with decreased aggregate stability under flow in response to iMer's inhibition of platelet-platelet binding (Figure 6B).

iMer delays washed human platelet spreading on fibrillar collagen visualized by SEM

Human WPs pretreated with vehicle demonstrated a greater proportion of activated platelets when exposed to fibrillar collagen, evidenced by a flattened, "fried egg" appearance, whereas those pretreated with iMer appear more commonly in the round resting state, similar to those treated with abciximab as a positive control (supplemental Figure 2). iMer-treated platelets exhibited an intermediate spreading phenotype compared with platelets treated with vehicle or abciximab.

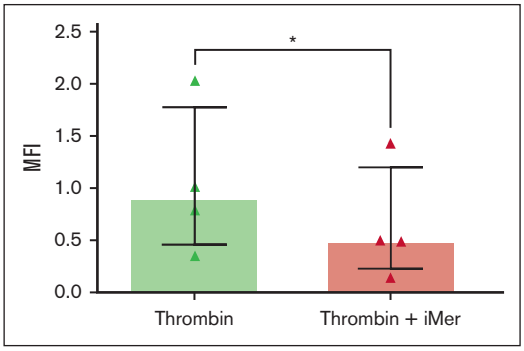

Figure 5. iMer inhibits platelet granule release stimulated by thrombin. Human WPs were exposed to 0.5 U/mL thrombin for 10 minutes after incubation with 5 μM iMer (red) or vehicle control (green) for 10 minutes. Median values and IQR from 4 experiments are shown (n = 4; P < .05, Wilcoxon signed pairs rank test). MFI, mean fluorescense intensity.

iMer increases survival in a collagen/epinephrine-induced pulmonary embolism model

Collagen and epinephrine were injected into wild-type C57BL/6 mice to induce pulmonary embolism. All mice injected with vehicle died of pulmonary embolism within 5 minutes of collagen/epinephrine injection. In contrast, ~35% of littermates pretreated with 60 mg/kg iMer (n = 9; P = .0025) were still alive 30 minutes after collagen/epinephrine (Figure 7). *Gas6*$^{-/-}$ mice (n = 6; P = .0085) were similarly protected from fatal thromboembolism.

iMer is not associated with increased tail bleeding time

Preliminary evaluation of tail-clip bleeding times demonstrated no significant difference between tail bleeding times in vehicle-treated C57BL/6 mice (median, 15 minutes [IQR, 11.53-15]; n = 8) and littermates treated with 60 mg/kg iMer (median, 6.57 minutes [IQR, 3.55-9.13]; n = 3; P = ns) or *GAS6*$^{-/-}$ mice (median, 14.75 minutes [IQR, 9.87-15]; n = 5; P = ns), as seen in Figure 7B.

Discussion

In this study, we first described iMer, a plasma-soluble naturally occurring MERTK isomer, and demonstrated that iMer binds to GAS6 and inhibits ex vivo platelet activation and in vivo thrombus formation, without associated increase in hemorrhagic effect. iMer bound GAS6 directly decreased platelet activation during low-dose ADP-induced aggregation similar to an anti-GAS6 antibody, inhibited granule release detected by platelet-surface P-selectin expression, and reduced stability of platelet aggregates under venous shear conditions in a microfluidic assay. iMer also improved survival in a collagen/epinephrine-induced pulmonary embolism model, without increasing hemorrhage in a tail-clip bleeding model.

Our findings are consistent with others demonstrating decreased platelet activation and thrombus formation in the setting of congenital[5,25,26] and/or pharmacologic[12,25,26] inhibition of GAS6-TAM signaling. In particular, the actions of iMer on platelet activation are similar to that seen with sMer, the soluble MERTK extracellular domain that also binds to GAS6, acting as a ligand trap,[13] and decreasing platelet-platelet binding by limiting the inside-out signaling that results in αIIb/β3 integrin activation. The lack of inhibition demonstrated by iMer in GAS6-depleted plasma supports our hypothesis of iMer's GAS6-trapping mechanism of action, because it has no inhibitory effect when no GAS6 is present to sequester during the preaggregation incubation. The GAS6-depleted plasma, however, still achieves aggregation percentages near that of normal PRP, likely due to small but sufficient amounts of GAS6 released by platelet α-granules[25-27] that, because of the timing conditions of the experiment, would not likely be trapped by iMer because it is not released until the agonist is added when the aggregation experiment is already underway.

Previous work demonstrated that AXL and TYRO3, but not MERTK, have an important role in platelet activation and thrombus formation via a pathway that regulates inside-out signaling.[28] iMer's mechanism of action, that of trapping GAS6, a ligand

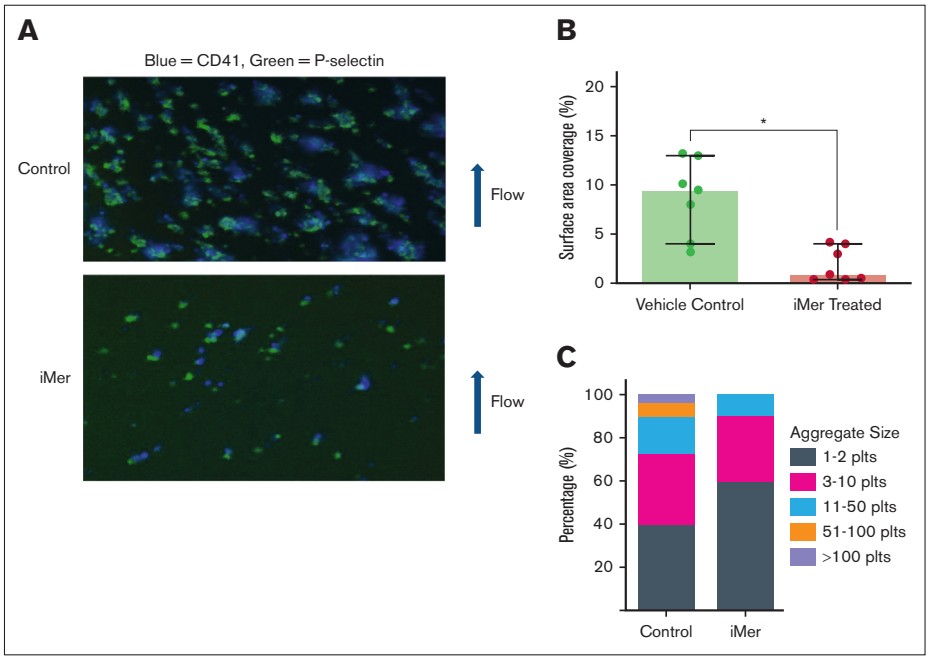

Figure 6. iMer inhibits stable aggregate formation under conditions of physiologic shear. (A) Human WB was pulled vertically (bottom to top) across horizontally oriented fibrillar collagen by vacuum syringe at a venous shear rate of 750 s^{-1}. Plts were stained with anti-CD41 antibody (blue), then counterstained with anti–P-selectin antibody (green). (B) Surface area coverage was calculated by densitometry and circularity measurements and was significantly higher in vehicle-treated human platelets (green, n = 7), compared with iMer-treated platelets (red, n = 7 independent experiment samples; $P < .05$, Wilcoxon signed pairs rank test). (C) Quantitation of brightfield images of platelets showing a higher proportion of small aggregates (1-2 and 3-10 platelets per aggregate) after pretreatment with iMer than samples pretreated with vehicle control, which contained higher proportions of large aggregates (11-50, 50-100, and >100 platelets per aggregate). plts, platelets.

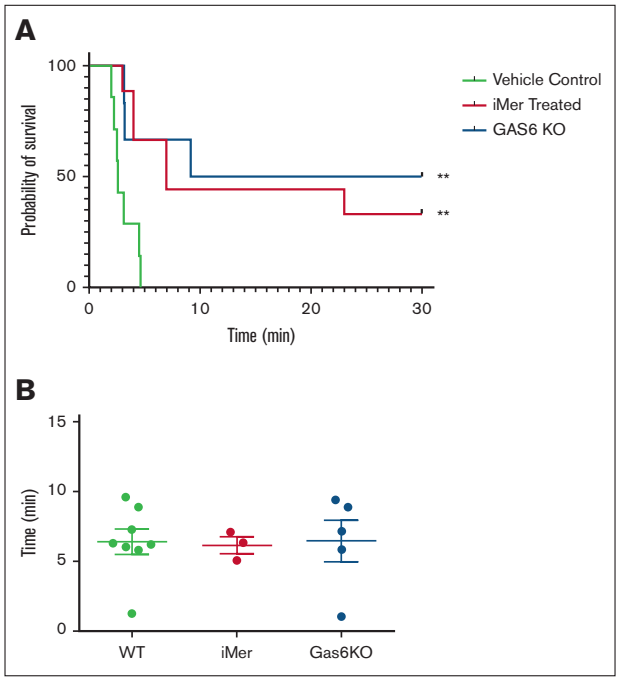

Figure 7. iMer protects against thrombus formation without increasing bleeding in preliminary studies. (A) C57BL/6 mice were injected with collagen/epinephrine to induce systemic venous thrombosis resulting in pulmonary embolism. WT mice treated with 60 mg/kg iMer (red, n = 9) and *Gas6*$^{-/-}$ KO mice (blue, n = 6) exhibited a significant increase in survival compared with vehicle-treated controls (green line; n = 7; $^{**}P < .01$ by log-rank [Mantel-Cox] test). (B) Tail-clip bleeding times did not differ significantly among WT mice treated with 60 mg/kg iMer (red, n = 3) or vehicle control (green, n = 8), or *Gas6*$^{-/-}$ KO mice (blue, n = 5; $^{**}P < .01$ by log-rank [Mantel-Cox] test). KO, knockout; WT, wild-type.

common to all TAM receptors, is still supported in light of these findings. Although iMer occurs naturally in mice and humans, the recombinant protein used here is labeled with a His tag to allow detection of exogenous protein. Differences in endogenous iMer levels may have contributed to differences in the efficacy of exogenous iMer in different donor samples. Another potential limitation is the preferential correlation of platelets more with arterial, rather than venous, thrombosis. More recent evidence, however, has linked platelet activation markers with venous thrombosis. Swamy et al demonstrated that plasma P-selectin levels were associated with increased risk of venous thromboembolism in females,[29] although it is not clear why men did not demonstrate the same risk elevation.

Our initial hypothesis that a naturally occurring, soluble splice variant of the MERTK receptor, would decrease platelet activation and thrombus formation is supported by our findings. These data implicate iMer as a potential strategy to decrease platelet activation and thrombosis risk, especially considering the lack of increased bleeding noted with iMer use. It remains to be seen whether iMer levels vary in certain situations, such as clinical inflammatory states, in which GAS6 levels are also elevated, to act more directly as a natural anticoagulant. Future studies should include direct measurement of the iMer product in samples from individuals with and without inflammation, for correlation with GAS6 levels.

Acknowledgments

The authors thank Peter and Deb Newman for helpful contributions to study design, data summary/analysis, and manuscript draft review. The authors greatly appreciate the manuscript review from Alan Mast.

This study was supported, in part, by a National Institutes of Health, National Heart, Lung, and Blood Institute 5K12HD068372-05 Institutional K12 award and K08HL46941 Mentored Clinical Science Research award; a Versiti Blood Research Institute Jackie Frederick Clinical Research award; a Versiti Comprehensive Center for Bleeding Disorders Joan Gill Pilot award; the Midwest Athletes Against Childhood Cancer Fund; the Children's Colorado Tanabe-Bobrow Family Young Investigator Award Endowed Fund and H30MC24049, Special Projects of Regional/National Significance, Maternal Child Health Bureau/Health Resources and Services Administration; a Hemostasis Thrombosis Research Society Mentored Research Award; an American Society of Hematology Scholar Award; a Takeda/National Hemophilia Foundation Clinical Fellowship Award; a CSL Behring Professor Heimburger Award (B.R.B.); and the University of Colorado's Postle Family Chair in Cancer and Blood Disorders (J.D.P.).

Authorship

Contribution: B.R.B. performed platelet function assay experiments and animal models, analyzed the data, and wrote the manuscript; S. Springborn, S.J., and A.K. performed platelet aggregation assays; S. Springborn generated primary figures; D.V. and P.M. performed immunoprecipitation and western blot protocols, and generated primary figures; C.B. and A.C. performed platelet aggregation assays and murine thrombosis models; S. Sather performed the tyrosine phosphorylation experiments and interpretation, and edited the manuscript; D.D. assisted with the $FeCl_3$ model and edited the manuscript; K.B.N. performed scanning electron microscope imaging, assisted with microfluidic flow assay and analysis, and edited the manuscript; D.K.G. and J.D.P. oversaw concept and design, provided equipment and reagents, and edited the manuscript.

Conflict-of-interest disclosure: J.D.P., D.K.G., and D.D. have stock in Meryx, Inc, a company developing novel anti-MERTK therapeutics. The remaining authors declare no competing financial interests.

ORCID profiles: K.B.N., 0000-0001-7546-4588; D.D., 0000-0002-7457-9006; B.R.B., 0000-0002-4076-270X.

Correspondence: Brian R. Branchford, Hemostasis and Thrombosis, Versiti Blood Research Institute, 8733 W Watertown Plank Rd, Wauwatosa, WI 53226; email: bbranchford@versiti.org.

References

1. Lozano R, Naghavi M, Foreman K, et al. Global and regional mortality from 235 causes of death for 20 age groups in 1990 and 2010: a systematic analysis for the Global Burden of Disease Study 2010. *Lancet*. 2012;380(9859):2095-2128.
2. Lemke G. Biology of the TAM receptors. *Cold Spring Harb Perspect Biol*. 2013;5(11):a009076.
3. Lew ED, Oh J, Burrola PG, et al. Differential TAM receptor-ligand-phospholipid interactions delimit differential TAM bioactivities. *Elife*. 2014;3:e03385.
4. Sasaki T, Knyazev PG, Clout NJ, et al. Structural basis for Gas6-Axl signalling. *EMBO J*. 2006;25(1):80-87.
5. Angelillo-Scherrer A, Burnier L, Flores N, et al. Role of Gas6 receptors in platelet signaling during thrombus stabilization and implications for antithrombotic therapy. *J Clin Invest*. 2005;115(2):237-246.
6. Law LA, Graham DK, Di Paola J, Branchford BR. GAS6/TAM pathway signaling in hemostasis and thrombosis. *Front Med (Lausanne)*. 2018;5:137.
7. Tibrewal N, Wu Y, D'mello V, et al. Autophosphorylation docking site Tyr-867 in Mer receptor tyrosine kinase allows for dissociation of multiple signaling pathways for phagocytosis of apoptotic cells and down-modulation of lipopolysaccharide-inducible NF-kappaB transcriptional activation. *J Biol Chem*. 2008;283(6):3618-3627.
8. van der Meer JH, van der Poll T, van 't Veer C. TAM receptors, Gas6, and protein S: roles in inflammation and hemostasis. *Blood*. 2014;123(16):2460-2469.
9. Prevost N, Woulfe D, Tognolini M, Brass LF. Contact-dependent signaling during the late events of platelet activation. *J Thromb Haemost*. 2003;1(7):1613-1627.
10. Nagata K, Ohashi K, Nakano T, et al. Identification of the product of growth arrest-specific gene 6 as a common ligand for Axl, Sky, and Mer receptor tyrosine kinases. *J Biol Chem*. 1996;271(47):30022-30027.
11. Chen C, Li Q, Darrow AL, et al. Mer receptor tyrosine kinase signaling participates in platelet function. *Arterioscler Thromb Vasc Biol*. 2004;24(6):1118-1123.
12. Branchford BR, Stalker TJ, Law L, et al. The small-molecule MERTK inhibitor UNC2025 decreases platelet activation and prevents thrombosis. *J Thromb Haemost*. 2018;16(2):352-363.
13. Sather S, Kenyon KD, Lefkowitz JB, et al. A soluble form of the Mer receptor tyrosine kinase inhibits macrophage clearance of apoptotic cells and platelet aggregation. *Blood*. 2007;109(3):1026-1033.
14. Hurtado B, de Frutos PG. GAS6 in systemic inflammatory diseases: with and without infection. *Crit Care*. 2010;14(5):1003.
15. Balogh I, Hafizi S, Stenhoff J, Hansson K, Dahlbäck B. Analysis of Gas6 in human platelets and plasma. *Arterioscler Thromb Vasc Biol*. 2005;25(6):1280-1286.
16. Borgel D, Clauser S, Bornstain C, et al. Elevated growth-arrest-specific protein 6 plasma levels in patients with severe sepsis. *Crit Care Med*. 2006;34(1):219-222.
17. Graham DK, Dawson TL, Mullaney DL, Snodgrass HR, Earp HS. Cloning and mRNA expression analysis of a novel human protooncogene, c-mer [published correction appears in *Cell Growth Differ*. 1994;5(9):1022]. *Cell Growth Differ*. 1994;5(6):647-657.

18. McCarty OJ, Calaminus SD, Berndt MC, Machesky LM, Watson SP. von Willebrand factor mediates platelet spreading through glycoprotein Ib and alpha(IIb)beta3 in the presence of botrocetin and ristocetin, respectively. *J Thromb Haemost*. 2006;4(6):1367-1378.

19. McCarty OJT, Larson MK, Auger JM, et al. Rac1 is essential for platelet Lamellipodia formation and aggregate stability under flow. *J Biol Chem*. 2005; 280(47):39474-39484.

20. Neeves KB, Maloney SF, Fong KP, et al. Microfluidic focal thrombosis model for measuring murine platelet deposition and stability: PAR4 signaling enhances shear-resistance of platelet aggregates. *J Thromb Haemost*. 2008;6(12):2193-2201.

21. Neeves KB, Onasoga AA, Hansen RR, et al. Sources of variability in platelet accumulation on type 1 fibrillar collagen in microfluidic flow assays. *PLoS One*. 2013;8(1):e54680.

22. Hansen RR, Wufsus AR, Barton ST, Onasoga AA, Johnson-Paben RM, Neeves KB. High content evaluation of shear dependent platelet function in a microfluidic flow assay. *Ann Biomed Eng*. 2013;41(2):250-262.

23. Westrick RJ, Winn ME, Eitzman DT. Murine models of vascular thrombosis (Eitzman series). *Arterioscler Thromb Vasc Biol*. 2007;27(10):2079-2093.

24. Branchford BR SS, Sather S, Brodsky G, et al. iMer blocks phosphorylation of the β3 integrin, decreasing platelet activation responses and protecting mice from arterial thrombosis [abstract]. *Blood*. 2011;118(21):189.

25. Angelillo-Scherrer A, de Frutos PG, Aparicio C, et al. Deficiency or inhibition of Gas6 causes platelet dysfunction and protects mice against thrombosis. *Nat Med*. 2001;7(2):215-221.

26. Cosemans JM, Van Kruchten R, Olieslagers S, et al. Potentiating role of Gas6 and Tyro3, Axl and Mer (TAM) receptors in human and murine platelet activation and thrombus stabilization. *J Thromb Haemost*. 2010;8(8):1797-1808.

27. Ishimoto Y, Nakano T. Release of a product of growth arrest-specific gene 6 from rat platelets. *FEBS Lett*. 2000;466(1):197-199.

28. Zhou J, Yang A, Wang Y, et al. Tyro3, Axl, and Mertk receptors differentially participate in platelet activation and thrombus formation. *Cell Commun Signal*. 2018;16(1):98.

29. Swamy S, Ueland T, Hansen JB, Snir O, Brækkan SK. Plasma levels of P-selectin and future risk of incident venous thromboembolism. *J Thromb Haemost*. 2023;21(9):2451-2460.